Science with the Hubble Space Telescope – II
Space Telescope Science Institute, 1996
P. Benvenuti, F. D. Macchetto, & E. J. Schreier, eds.

The Birth of Stars: Herbig-Haro Jets, Accretion and Proto-Planetary Disks

John Bally[1] and Jon Morse

Campus Box 389, Center for Astrophysics and Space Astronomy, University of Colorado, Boulder CO 80309, USA

Bo Reipurth

European Southern Observatory, Casilla 19001, Santiago, Chile

Abstract. On the 200th anniversary of the publication of Laplace's theory for the birth of the Solar System, we finally have the tools needed to directly observe the formation of stars and planets. We can observe the star formation process at virtually all wavelengths of the electromagnetic spectrum from X-rays to radio wavelengths. The Hubble Space Telescope (HST) provides us with the highest angular resolution tool with which to investigate the jets produced by stars during their birth and the circumstellar accretion disks where we believe planets might form.

1 Overview of Star Formation

Stars are born in the dense cores of 10^4 to 10^6 $M_\odot$ giant molecular clouds (GMCs). The total mass of molecular gas in the Galaxy is about 2 to 4 $\times 10^9$ $M_\odot$ and there is a comparable amount of atomic hydrogen (HI). Thus, the total reservoir of interstellar gas that is available for star formation is about 5×10^9 $M_\odot$, a few percent of the baryonic mass of the Milky Way. Stars are forming at an average rate of about 3 $M_\odot$ yr^{-1} throughout the Milky Way from this gas.

GMCs are supported against global gravitational collapse by magnetic fields and MHD turbulence. Gravitational collapse of molecular cloud cores can occur via two distinct modes (see Shu et al. 1993 and references therein). *Magnetic supercritical collapse* occurs when a sufficient density of material accumulates in a given region so that the inward pull of gravity overwhelms the outward pressure of magnetic fields. For mean GMC parameters near the Sun, this tends to occur on mass scales of order 10^3 $M_\odot$. Fragmentation must produce ultra-dense sub cores of stellar mass. Collapse can also occur via *ambipolar diffusion* which occurs more slowly as neutrals slip through the magnetic field (and the ions and electrons coupled to it), lowering the mass where collapse sets in to about 1 $M_\odot$.

Millimeter wavelength observations of nearby GMCs show that the cloud cores in which stars form range from 1 to more than 1000 $M_\odot$. Most cores produce ultra-dense but *transient clusters* of stars (Lada et al. 1991a,b, Lada, Strom, & Myers 1993). Although some star formation occurs in isolated small clouds and globules which may have collapsed through ambipolar diffusion or by external compression, isolated star formation is relatively rare in the solar vicinity (Reipurth 1983). Out of the approximately 10^5 stars formed in the past 10^7 years within a distance of 500 pc from the Sun, most were formed in transient clusters in the major OB associations (Orion OB1, Perseus OB2, and the Sco-Cen OB Association). Thus, the supercritical collapse mode may dominate star formation. For instance, in Orion, most of the young stars are concentrated into 7 to 8 *transient* clusters containing between 50 and 700 stars each typically in a volume much smaller than a cubic parsec. The Trapezium cluster lying at the heart of the Orion Nebula has a central density of young

[1] Astrophysical, Planetary, and Atmospheric Sciences Department, University of Colorado, Boulder

stars of about 50,000 stars per cubic parsec (McCaughrean & Stauffer 1994). Some stars are born in relatively isolated environments such as the Taurus dark clouds. Even in the dark clouds however, star formation is highly clustered. In the L1551 core in Taurus, over a dozen stars were born in the past 10^6 years, in a region that has a diameter of only several tenths of a parsec.

Such dense star clusters do not survive for much longer than a stellar crossing time. They usually dissolve in less than 10^6 years because the efficiency of star formation (mass of stars formed / initial available mass of gas) is around 5 to 15%. Young stars typically move with a random velocity that is close to the initial escape velocity from a cloud core, and if more than 70% of the initial gas mass is removed (by ionization or the impact of stellar outflows), the cluster will evaporate. The formation of *bound* star clusters requires that more than about 30% of the initial mass in a collapsing core be converted to stars. From the number and ages of galactic open clusters, this must occur infrequently; the bound open cluster formation rate is less than 2 to 4 per square kpc per every 10^7 years (Battinelli & Capuzzo-Dolcetta 1991).

Stellar mass fragments in gravitationally collapsing GMC cores typically develop specific angular momenta (angular momentum per unit mass) about 5 orders of magnitude larger than that of stars through mutual tidal interactions between adjacent cores or by other differential forcing. Such rotating cores collapse into disks, which through dissipation of their angular momentum, accrete mass onto a central proto-star.

Most models of young stars and their immediate environments incorporate magnetic fields. Magnetic fields in the collapsing, rotating cloud core are advected with the accretion flow and form an hour glass shaped B field that is pinched inward by the forming disk. The accreting central proto-star, which becomes fully convective soon after its formation, supports a rigid, co-rotating (with the star), roughly di-polar stellar field which may extend to 5 to 10 stellar radii. The point where the outermost stellar field line intersects the accretion disk determines the rotation rate of the young star. This point will rotate with the Keplerian rotation speed of the disk at that radius. Inside this radius, the stellar B field dominates all pressures and rotates as a rigid body anchored to the star. Matter is picked up from the disk, forced to move along magnetically dominated accretion columns to high stellar latitudes, where it is accreted onto the star. Most workers have adopted this magnetic geometry, first worked out by Ghosh & Lamb (1977,1978). In this scenario, the magnetic X point where the stellar field intersects the disk is the point of origin of a magneto-centrifugally driven wind fueled by matter injected onto open field lines and flung to infinity (Lovelace et al. 1995, Wardle & Königl 1993, Shu et al. 1994, Ostriker & Shu 1995). In this picture, magnetic forces on the open field lines 0.1 to 10 AU from the central star are responsible for collimating the wind into a stellar jet.

Many theoretical aspects of this model are incomplete. Observations make it clear that stellar accretion, and mass loss from the young star or its disk, are highly variable. Models to date have not incorporated the full range of possible time-dependent behaviors expected of such a system.

What removes most of the initial mass of gas in a core and brings star formation to a halt? If massive stars are formed, UV radiation, stellar winds, and supernova explosions dissociate, ionize, heat, and accelerate remaining gas to speeds in excess of the escape velocity from the region. When only low mass stars form, residual gas may be dispersed by the impact of mass outflows and jets.

2 The Jets of Herbig and Haro

Almost 50 years ago, George Herbig and Guillermo Haro independently discovered a number of compact nebulae with peculiar spectra near dark clouds. Schwartz (1975) and Raymond (1979) demonstrated that these objects were shock-excited nebulae. Later workers showed that the large range of excitation conditions requires bow shocks and other complex morphologies. By the early 1980s, several Herbig-Haro (HH) objects were shown to be highly collimated jets of partially ionized plasma moving away from young stars at speeds of 100 to over 1000 km s^{-1}.

Today, well over 300 individual HH objects or groups are known (Reipurth 1994). Many individual HH objects consist of separate knots or bow shocks, others consist of highly linear chains

or jets. Most show evidence of being a part of or excited by a highly collimated flow from a young star.

Because star formation is highly clustered, HH flows also tend to be found in groups. Bally, Devine, & Reipurth (1996) have found a "burst" of HH objects emerging from the NGC 1333 region of the Perseus cloud. In addition to the previously known HH objects (HH 4 through HH 18), 21 new clusters of HH objects were found in a 20′ (2 pc) diameter area. At least 5 of the HH objects are parts of highly collimated stellar jets. When all of the substructure is taken into account, this field contains several hundred individual shocks, produced by several dozen active outflows from about 100 low mass young stars that have recently formed from this cloud core. A large portion of the surface area of the NGC 1333 cloud core is covered by visible shocks, demonstrating that such shocks, produced by outflows from low mass young stars, must have a profound impact on the surrounding environment.

By the early 1980s, millimeter wavelength observations of carbon monoxide (CO) revealed over 50 bi-directional, axially symmetric, but poorly collimated *molecular outflows*, of moderate velocity (3 to 100 km s^{-1}) CO bearing gas (Lada 1985, Fukui et al. 1993). We now believe that HH objects and CO outflows are different manifestations of the mass loss produced during star formation. Most nearby CO outflows, when inspected with sufficient sensitivity, are found to contain HH objects or shock-excited near infrared emission lines. Observations and models indicate that the high velocity jets ejected by young stars are the source of energy for HH objects with increasingly complex morphologies farther from their central sources. When such jets interact with molecular gas in their surroundings, they accelerate CO bearing gas. In some cases, the high pressure post-shock cooling layers can be sufficiently dense so that molecule formation time scales are comparable to dynamic time scales. Under such conditions, which are found close to the driving sources of the youngest stars, where internal working surfaces are formed by the interaction of faster jet fluid elements moving into slower fluid elements, clumps of very high velocity molecules can be formed. These may be the so called molecular "bullets" observed in jet-like molecular outflows such as L1448C, IRAS03282, and HH 111.

2.1 Significance of HST Observations of Jets

It is apparent that outflows from young stellar objects are an integral part of the star formation process. Most stars undergo a phase that lasts for over 10^5 years during which energetic mass loss occurs in the form of numerous eruptions. These jets may become less collimated with increasing age. Jets have ejection velocities of order several hundred kilometers per second for low mass stars, and in excess of 10^3 km s^{-1} for high luminosity sources that will evolve into O, B, and A stars. Jet densities range from n = 10^2 to over 10^5 cm^{-3}, and the ionization fractions vary from way below 1% to 10%. The shock cooling times are short (few to thousands of years), which lead to a very rich variety of structures resulting from a combination of cooling and hydrodynamic instabilities (Visniak and Rayleigh-Taylor instabilities; see Stone et al. 1995) and time dependent variations in the outflow parameters. The multiple bow shocks and S-shaped point symmetry seen in some sources almost certainly requires variations in the mass ejection velocity to produce internal working surfaces and precession or irregular wobbling of the jet.

Many outflows can be traced for parsecs from their exciting sources. HST has been used to image the bright inner portions of these outflows, where the flow takes the form of a jet. The HST observations with their 0.05 to 0.1″ angular resolution, resolve for the first time the cooling length in some shocks in Herbig-Haro flows. In some flows there is evidence for Balmer-line shocks traced by pure Hα emission that are well separated from the downstream cooling regions. With HST, we can measure the proper motions of individual knots on exposures taken less than a year apart. Since the time required to measure the proper motions is likely to be less than the cooling time, it should be possible for the first time to uniquely disentangle true proper motion from photometric variability resulting from intensity variations due to the cooling of distinct fluid elements.

Protostellar jets appear to evolve into parsec scale outflows which may dominate the injection of kinetic energy, dissociation of molecular gas, and generation of supersonic turbulence in GMCs

in those portions of the cloud where only low to intermediate mass stars are forming. A detailed understanding of the behavior of these jets may be vital to our understanding of the large-scale properties of molecular clouds.

Stellar jets in the HST era can be used as "laboratories" to verify our models of the hydrodynamic (and MHD) evolution of jets by direct comparison with data. Stellar jets are sufficiently near so that we can measure proper motions, radial velocities, the location of components on the plane of the sky with high angular resolution, and the time dependent behavior of the jets. This is the only category of supersonic astrophysical jets where we can measure 5 out of the 6 phase space dimensions of a flow!

Jets and outflows record the recent mass ejection history of their driving sources. For the parsec scale jets, the outermost shocks are typically 5×10^3 to 5×10^4 years old, about a factor of 2 to 20 less than the estimated total duration of the proto-stellar jet phase. HH objects lying farther from the source trace gas ejected earlier. From the analysis of the total mass, flow velocity, and ejection direction, we may be able to reconstruct the history of recent mass loss, and by inference, the accretion history of a young star.

The ultimate goal of research on jets is to probe the nature of physical processes that operate within several AU of a young star, to learn about the potential existence of physical conditions that might lead to the formation of planets, and to understand how stars and planetary systems form.

We now review in some detail the outflows from 3 young stars. We will discuss ground-based and HST observations of the HH 34, HH 111, and HH 46/47 systems.

2.2 The HH 34 System

The lower left panel of Figure 1 shows a narrow band image (in Hα + [S II]$\lambda\lambda$6716, 6731 emission) of the HH 34 (Reipurth et al. 1986) jet obtained by Jeff Hester and the WFPC I team. The young star driving this outflow is located to the upper right of the slender jet, that appears as a chain of knots, which upon close inspection consists of a train of bow shocks. Ground-based spectra and proper motions show that the individual knots in the jet are moving away from the source at about 220 to 250 km s^{-1}, and the jet is inclined about 20^o to 30^o from the plane of the sky. The low excitation emission indicates very low shock velocities in the knots, which must be internal working surfaces within the jet where slight flow velocity variations are producing shocks. The jet becomes much fainter about 30″ from the source. About 90″ south of the central star, there is a spectacular bow shock, where the jet encounters much slower moving neutral material. The bow is bright in Hα and has [O III] emission at its apex. The shock propagating back into the decelerating jet (the reverse shock) is bright in [S II] emission. Thus, the bow shock is stronger than the reverse shock, indicating that the jet material is much denser than the pre-shock medium. The bow shock is corrugated and wavy, indicating that instabilities may be starting to develop or that the pre-shock medium is inhomogeneous.

Ground-based images show that the HH 34 jet is only the inner part of a complex outflow that can be traced for over 10′ on both sides of the central young star (Bally & Devine 1994—see Figure 1). HH 34 itself is the first in a chain of increasingly complex bow shocks lying to the south. Next in line are HH 34X, HH 172, HH 86, HH 87, and HH 88. Spectroscopy and proper motions show that all of these bow shocks are moving to the south and are blue shifted. There is a systematic decrease in the amplitude of the velocity vector with increasing distance from the source. There is also a systematic increase in the degree of fragmentation and morphological complexity of the bow shocks with increasing age and distance from the source, indicating the growth of non linear thermal or dynamic instabilities. To the north, there is a counter-chain of shocks, starting with HH 34N, and containing HH 126, HH 85, and ending in HH 33/40. All of these objects are moving approximately northward and have red shifted velocities. Overall, the HH 34 system exhibits S-shaped point symmetry about the central source, indicating that over the 5000 year life of the most distant HH objects, the ejection direction of the jets has precessed or wobbled by an angle of order 5^o or 10^o.

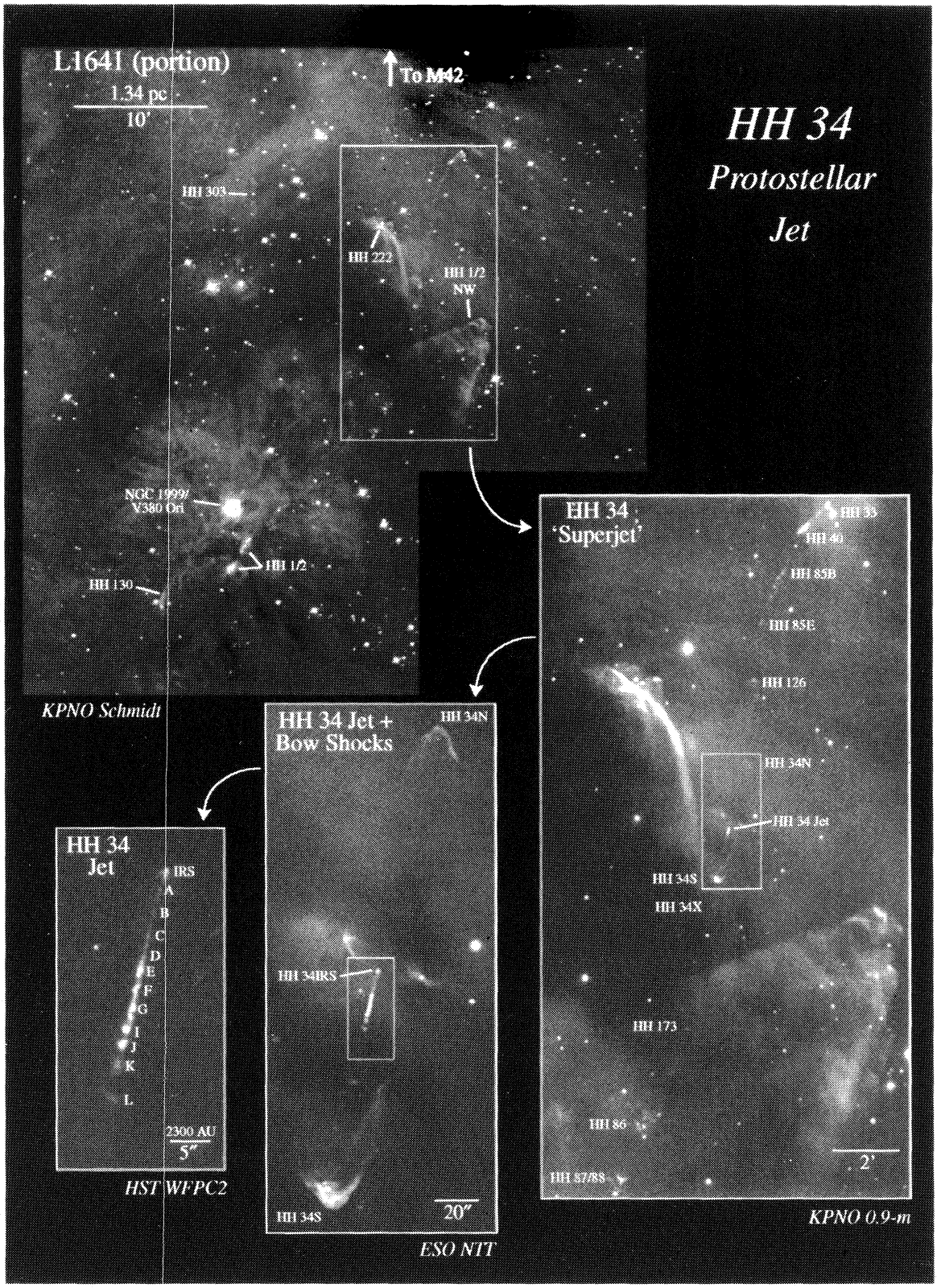

Figure 1. Ground-based and HST images of Hα+[S II] in the HH 34 system. A scale indicates the relative size of each frame. *Upper left.* KPNO 0.6 m Schmidt. *Lower right.* KPNO 0.9 m. *Lower middle.* ESO 3.5 m NTT *Lower left.* HST WFPC2

The HH 34 system is associated with only a weak CO outflow (Chernin & Masson 1995) that is confined to the inner arc minute nearest the driving young star. We know from the low obscuration of the shocks in this system that this outflow must lie near the front face of the L1641 molecular cloud in the southern portion of the Orion OB association. The jet may be mostly ramming atomic gas, except in the immediate vicinity of the remnant cloud core that surrounds the HH 34 driving source.

HH 34 was the first optical outflow with a highly collimated jet from a young low-mass star that was recognized to have a spatial extent of more than one parsec. Over 20 parsec-scale outflows have been recognized within the past year, mostly as a direct consequence of the availability of large format CCDs (Reipurth, Bally, & Devine 1996).

2.3 The HH 111 System

HH 111 (Reipurth 1989) is the driving jet of a seven parsec long outflow from a cometary globule located in the northeastern edge of the Orion superbubble. Figure 2 shows ground-based and HST images made using narrow band Hα and [S II] filters.

As with HH 34, internal shocks cause the jet to light up along much of its 140″ length. The source of the jet is a young star just off the left edge of the HST image. It is completely obscured at visual wavelengths by a thick disk of circumstellar matter. The jet becomes visible about 5″ west of the source where the extinction drops to sufficiently low values. Working from left to right (from the source towards the west), the jet at first appears to narrow just at the location of an Hα bright bow shock. For about 30″, the jet resembles a tube with a nearly constant width of about 0.5″ containing [S II] bright material. The surface of this tube contains about a dozen knots or arcs of [S II] emission. Most of these features are associated with arcs of Hα emission that lie ahead of their [S II] counterparts by several pixels (0.1″to 0.3″). Some of these Hα wisps extend beyond the [S II] bright portion of the jet (orthogonal to the jet axis). Most do not form complete bow shocks but appear cometary or one-sided. There is a hint of a helical pattern in the [S II] bright arcs, especially near the downstream end of the jet. These may be transverse shocks produced by slight wiggling of the jet about its mean axis that causes some of its material to shock against a slower moving sheath or cocoon of gas, or partial bow shocks produced by low amplitude velocity variations in the jet. About 60″ from the source, the jet expands as the [S II] emission fades, leaving behind a chain of Hα bright and more or less complete bow shocks. The axis of symmetry of these bows alternates from above the jet to below the jet. Finally, a large bright bow shock (HH 111V) is located at the right edge of the HST image. Faint filamentary emission fills the region between HH 111V and the brightest portion of the jet.

Ground-based wide field narrow band CCD images show that HH 111 is the bright inner portion of a 7 parsec long outflow that terminates in HH 311 located about 35′ to the west (Winkler & Reipurth 1992) and in HH 113, located 25′ to the east, with additional HH knots located between these terminal bow shocks and the HH 111 jet (Reipurth, Bally, & Devine 1996). As with the HH 34 system, all shocks are found to be moving away from the HH 111 source with a velocity that systematically decreases with increasing distance from the source, from over 500 km s^{-1} in HH 111, to under 100 km s^{-1} in HH 311 and HH 113.

A compact high velocity CO outflow was found by Reipurth & Olberg (1991) to be associated with the HH 111 cloud core and the visible jet. Recent millimeter interferometer data show that the jet itself contains high velocity CO, and that the bright bow shock (HH 111V) is associated with a 10^{-4} $M_\odot$ knot of CO that is moving at the same radial velocity measured for the visual emission (Cernicharo & Reipurth 1996). The CO data also shows a chain of high velocity 'bullets' to the west of HH 111V where no optical emission is seen. The HH 111 jet appears to be inclined by only 10^o with respect to the plane of the sky, so the observed 90 km s^{-1} radial velocity of the CO implies that this gas is actually moving at 500 km s^{-1}, a speed comparable to the fastest optically bright components of the jet. These observations indicate that not only is the jet mostly neutral, but that it contains molecular gas. The existence of a sheath of lower velocity CO surrounding the jet provides evidence for entrainment of molecular gas from the host cloud by entrainment (De Young

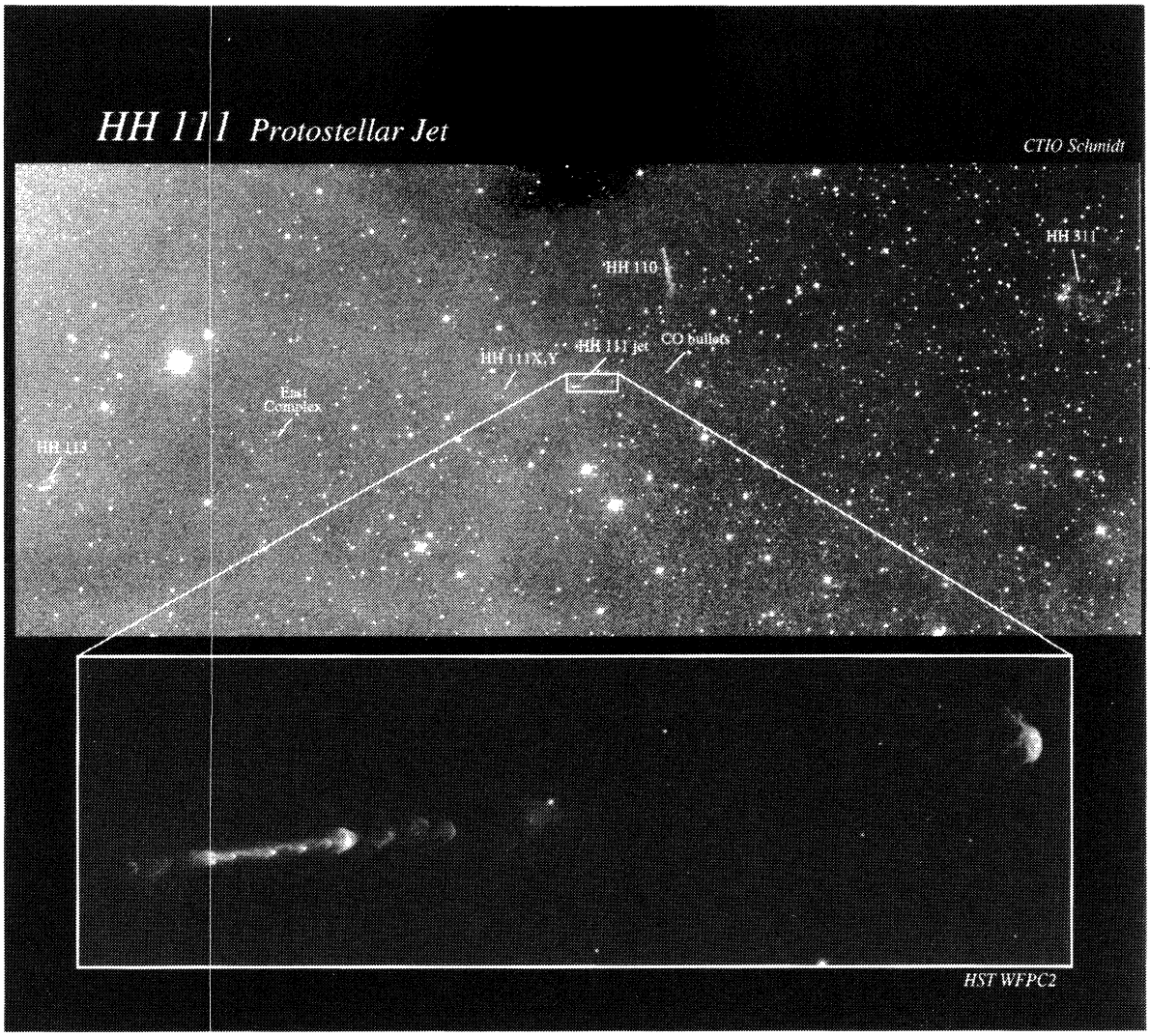

Figure 2. The HH 111 system. The top panel shows a 1 degree field-of-view CTIO 0.6 m Curtis Schmidt image that shows the terminal bow shocks (HH 113 and HH 311) at the ends of the outflow. The location of HH 111 is indicated by the rectangle near the middle of the image. The bottom panel shows the HST image of the HH 111 jet. [S II] is red and Hα is cyan.

1986) and a medium into which the transverse Hα wisps observed by HST may be propagating, perhaps accelerating the CO bearing gas. The presence of very high velocity 'bullets' of CO in HH 111V and beyond, as well as 2.1μm H_2 emission in some jet knots (Gredel & Reipurth 1994), indicate that molecules may reform after gas has passed through a shock.

2.4 The HH 46/47 System

HH 46/47 is one of the first HH jets to be recognized (Schwartz 1977, Dopita et al. 1982). Located in a small cometary globule in the Gum Nebula, it may be one of the relatively rare examples of isolated star formation where only a single star is produced (Reipurth 1983). Figure 3 shows a [S II] bright jet extending from a reflection nebula (that contains HH 46) illuminated by an embedded young star. The jet extends towards the northeast where it terminates in a bright knot (HH 47A) located 70″ from the IR source. A large but fainter bow shock lies 40″ farther to the northeast (HH 47D). A faint counter jet can be seen through a hole in the globule to the southwest of the

young star. A faint bow shock (HH 47 C) can be seen emerging from behind the globule about 110″ to the southwest of the central source, directly opposite (with respect to the central young star) to the position of HH 47D.

As with the other jets discussed above, a molecular outflow is associated with the inner regions of HH 46/47. However, since the blue shifted lobe of the jet appears to be blowing into the mostly atomic or ionized gas lying in the interior of the Gum Nebula to the northeast while the red shifted counter jet is blowing back into the molecular globule, the CO flow is mostly red shifted, with only a very faint blue shifted component (Chernin & Masson 1991). As with HH 111, portions of the outflow are detected in near infrared 2.122 μm H_2 emission. However, in this case this emission in confined to the knot HH 47A, the counterjet, and to the walls of a bubble of gas that appears to be a near infrared extension of the wings of the HH 47C bow shock (Eisloeffel et al. 1994). Morse et al. (1994) present velocity resolved Fabry-Perot data cubes for the Hα and [S II] emission from the HH 46/47 flow which show that the jet cocoon has a much lower radial velocity than the jet itself.

The inset of Figure 3 shows an HST image of the blue shifted portion of this outflow in Hα and [S II] emission (Heathcote et al. 1996). As with HH 111, a series of one-sided bow shocks can be seen extending from the sides of the jet. The jet itself is bright in [S II]. In addition to knotty and turbulent looking [S II] emission, a series of wisps of Hα emission extend from the main body of the jet into the cocoon of material that surrounds it. These wisps are generally devoid of [S II] emission (the ratio of Hα/[S II] is at least 40). We interpret these sharp, curved Balmer line filaments as emission that is tracing the heating layer where mostly neutral gas entering the shock is collisionally excited and radiates prior to becoming fully ionized and invisible. Since this layer is only a few collision lengths thick, only hydrogen can radiate. Other trace ions or atoms radiate in proportion to their abundances and are too faint. The detection of pure Hα emission indicates that we have resolved the shock structure. We can cleanly separate the shock from the recombination layer which is separated by nearly 1″ in several of the transverse wisps.

The HH 47A bow shock is fully resolved. We can recognize the reverse shock ("Mach disk") into the jet, the forward facing bow shock, and the post shock cooling layers trapped between. The bow shock can be traced for over 20″ from its apex. A faint skin of Hα bright emission wraps around HH 47A. It expands laterally (transverse to the jet) for about 3 to 6 times the radius of the jet, after which this structure is swept back and remains parallel to the jet. Such extended bow shock wings and perhaps the one-sided jet shocks in the jet may be the sites of CO acceleration where molecular outflows are produced.

3 Externally Illuminated Accretion and Proto-Planetary Disks

We (Bally, Devine, & Sutherland 1996) have used HST in Cycle 4 to obtain high angular resolution follow-up observations of the proto-planetary disks surrounding young stars embedded in the Orion Nebula that were discovered in the seminal observations of C. R. O'Dell and collaborators (O'Dell et al. 1993, O'Dell & Wen 1994). We have used the PC portion of WFPC2 to obtain 0.05″ images in the visible, FOC to push the angular resolution close to 0.02″ on a few objects, and FOS to obtain the first UV spectra.

The Trapezium region in the Orion nebula contains about 700 stars with a core density of 5×10^5 stars per cubic parsec. More than half are now embedded in the H II region ionized by the O6p star θ^1C Orionis. This star is the source of a powerful isotropic stellar wind with a mass loss rate of about $\dot{M} = 10^{-7}\ M_\odot\ yr^{-1}$ at a wind velocity that has been estimated to lie between 500 and 1500 km s^{-1}.

Young low mass stars (that formed along with the high mass stars responsible for the Orion nebula) are now exposed to an intense radiation field, and for stars lying within the stellar wind cavity, also a massive stellar wind. Fitting the low mass YSOs on an HR diagram (Herbig & Terndrup 1986) indicates that the median age of stars in the Trapezium cluster is only about 3×10^5 years. Many of these young stars have retained a portion of their circumstellar environments, permitting us to study this dense gas and dust with the unprecedented angular resolution of HST.

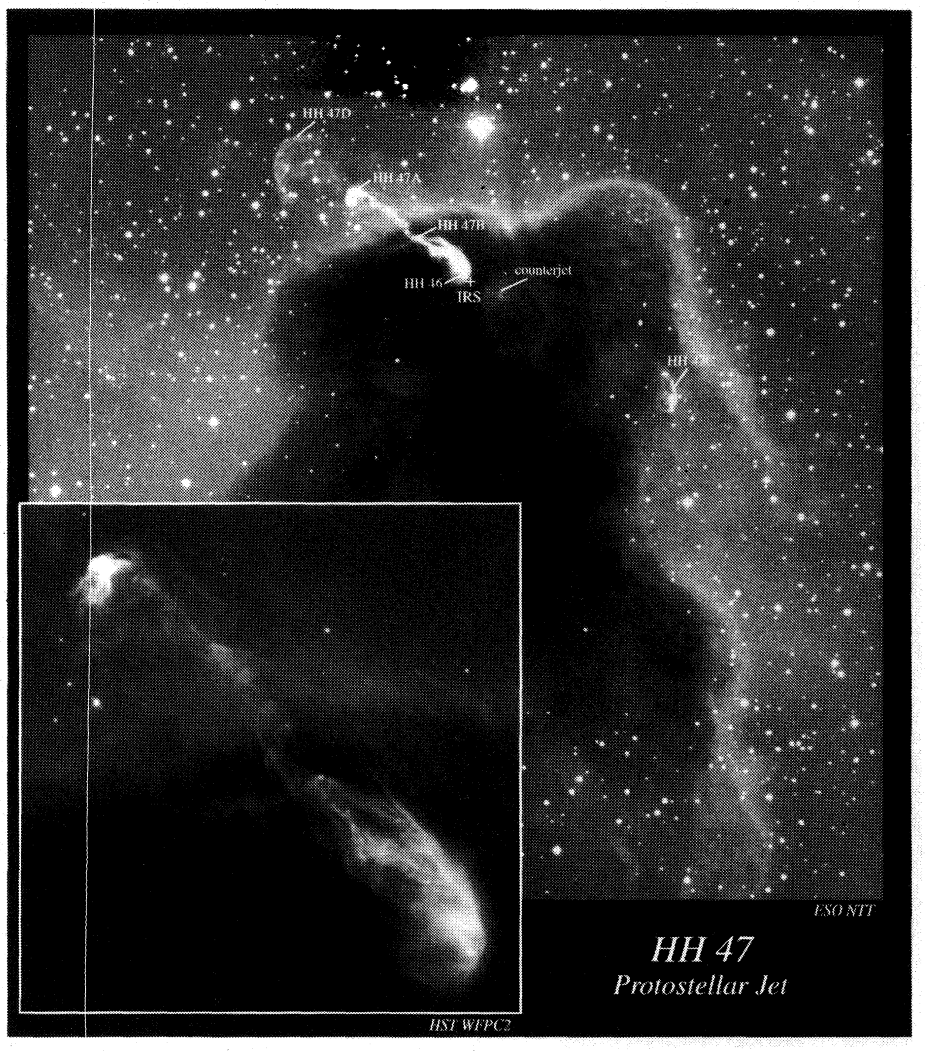

Figure 3. Ground-based and HST images of the HH 46/47 system. *Background.* 3.5 m ESO NTT. *Foreground.* HST WFPC2. [S II] in red and Hα in cyan.

Although millimeter wavelength interferometry had already detected Keplerian rotation in a number of disks surrounding nearby T-Tauri stars, these observations are limited in angular resolution to about 1″, corresponding to a linear scale of about 100 AU or more. There is some evidence that most of the usual millimetric tracers (CO, CS, etc) may be heavily depleted by either condensation onto grains, or by chemical processing, in the inner disks where planets may be forming and where proto-stellar jets must originate.

HST may provide the best available probe of conditions in the inner 100 AU of a proto-planetary disk. Photo-ablation of the low density envelope surrounding a YSO embedded inside an HII region removes the obscuring material that normally hides the accretion disk that surrounds a YSO. External illumination by nearby massive stars, or back-lightning by the ionized gas, permits us to study the structure of such disks with unprecedented angular and linear resolution ($< 0.03''$ or 15 AU in Orion) at UV and visual wavelengths.

Observations of the inner regions of the Orion Nebula by our and C. R. O'Dell's programs have shown that at least 150 stars in the inner region of the Orion Nebula contain extended circumstellar environments. Consideration of the physical processes involved indicates a sequence of expected morphologies with increasing distance from θ^1C Ori. Stars lying within the inner stellar wind bubble

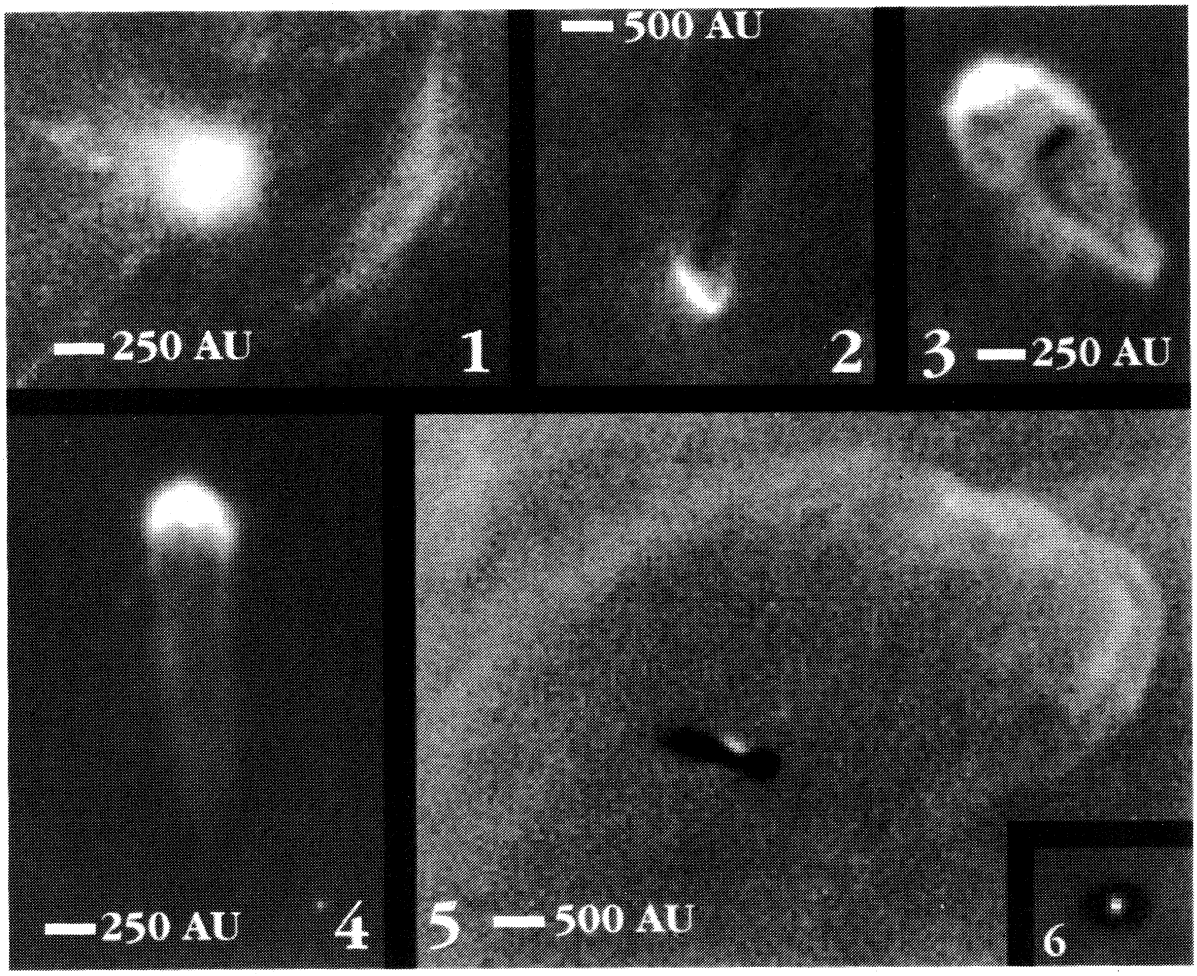

Figure 4. HST image showing six externally illuminated young stellar objects embedded in the Orion Nebula. Objects 1 and 4 (HST 1) lie within 30″ of the Trapezium, and probably are located inside the stellar wind bubble produced by θ^1C Ori. In colliding with the ionized gas photo-ablating from the cometary object, the stellar wind from the hot star may produce the shock excited [O III] arc (green) lying to the right of object 1. Objects 2 and 3 (HST 10) lie over 60″ from the Trapezium, probably outside the stellar wind bubble. A nearly edge-on disk inside the teardrop shaped HST 10 hides its central star. Objects 5 and 6 (HST 16) lie in front of the H II region outside the ionization front and are seen in silhouette against the nebular background. The the large green bubble around object 5 appears to be an HH object. As in HST 10, the central star is hidden by a nearly edge-on disk. However, starlight is scattered from the top surface of the disk towards our line of sight.

are first exposed to ionizing UV. The gas that is evaporated from the YSO circumstellar environment expands at approximately the sound speed in ionized gas and shocks against the stellar wind. Young stellar objects within 30″ of the hottest star in the Trapezium (θ^1C Ori) have arcs of [O III] and Hα emitting gas several arc seconds from the YSO (object 1 in Figure 4). Ground-based spectra show that at least some of these features are associated with high radial velocity gas, consistent with the wind shock model. Soft non-ionizing UV can penetrate the ionization front on the side of the YSO environment that faces θ^1C Ori. The radiation can couple strongly to the grains, dragging them through the gas, effectively straining (removing dust from) the gas that expands through the ionization front. The dust is driven radially away from the hot star, forming the spectacular cometary

tails seen in the objects near the Trapezium. From the surface brightness of the ionization front and the radio free-free flux, it is estimated that the typical mass loss rate of each YSO environment is about 10^{-7} $M_\odot$ yr^{-1} so that if the environment contains 0.01 $M_\odot$, it can survive for about 10^5 years.

For YSOs located outside the ram pressure (n_{wind} proportional to r^{-2}) dominated portion of the stellar wind bubble, the [O III] arcs disappear (object 2 in Figure 4). Since the intensity of radiation diminishes with increasing distance from the Trapezium, dust tail production also becomes less significant, and the ionization fronts that form around these young stars take on a tear-drop shape determined by the ratio of direct to scattered nebular UV ionizing continuum (object 3 = HST 10 in Figure 4). Circumstellar disks present inside the photo-ionization fronts surrounding the young stars produce silhouettes against the background nebular light (object 3 = HST 10 in Figure 4). Silhouettes are seen both in the cometary objects near the Trapezium, in the teardrop shaped objects located far from the Trapezium but still located inside the photoionized nebula, and in YSOs completely outside the Orion Nebula's Strömgren sphere, where no ionizing radiation can penetrate, and no ionization fronts are produced (objects 5 and 6 in Figure 4). At least 6 completely dark silhouettes have been found.

These observations demonstrate that circumstellar disks are common among low mass young stars. HST is providing us with the highest angular resolution probes of these disks. We hope that with more observations in the next few years, we can do the ultimate job in diagnosing the conditions in these proto-planetary environments, and perhaps detect indirect signatures of on-going planet formation.

4 Future Prospects

Future HST observations with WFPC2 will measure proper motions in jets already observed and will be used to study other examples of jets from young stars. With NICMOS, sub-arcsecond near infrared imaging of shock excited H_2 and [Fe II] will provide powerful new diagnostics of the innermost portions of outflows from young stars.

New UV, visual, and near infrared imaging and spectroscopy of the externally illuminated disks embedded in the Orion Nebula and other nearby HII regions will provide the best available probes of the structure of proto-planetary environments and the possible occurrence of planetary accretion. Are environments such as those found in the Orion Nebula unique? Indications are that most stars are born inside very dense transient proto-stellar clusters. In such clusters, most of which form in OB associations, nearby O and B stars will influence the evolution of low mass YSOs. Many (if not most) field stars may have been processed through harsh environments similar to those now observed near the Trapezium during the first few million years of their lives.

Thus, HST is playing a crucial role in understanding our own origin.

Acknowledgments. We thank our collaborators on the HST 'proto stellar jets' team, Pat Hartigan, Dick Schwartz, John Raymond, Jim Stone, and Steve Heathcote for their contributions. J. Bally gratefully acknowledges the collaboration of C. Robert O'Dell and Mark McCaughrean on the HST investigations of externally illuminated proto-planetary environments in the Orion Nebula. Special thanks to David Devine and Ralph Sutherland who played crucial roles in the analysis of ground-based and HST Orion Nebula data. This research was funded by NASA grants NAGW-4590, NAGW-3192, and HST grants GO-5469-93A and GO-5504-93A.

References

Bally, J., Devine, D., & Reipurth, B. 1996, ApJ, in press

Bally, J., Devine, D., & Sutherland, R. 1996, ApJ, in preparation

Bally, J. & Devine, D. 1994, ApJ, 428, L65

Battinelli, P. & Capuzzo-Dolcetta, R. 1991, in *The Formation and Evolution of Star Clusters*, ed. K. Janes, PASP Conf. Ser., Vol 13, p. 139

Chernin, L. M. & Masson, C. R. 1995, ApJ, 443, 181

Chernin, L. M. & Masson, C. R. 1991, ApJ, 382, 93

Cernicharo, J. & Reipurth, B. 1996, A&A, in press

DeYoung, D. 1986, ApJ, 307, 62

Dopita, M.A., Schwartz, R.D., & Evans, I. 1982, ApJ263, L73

Eisloeffel, J., Davis, C. J., Ray, T. P., & Mundt, R. 1995, ApJ, 422, L91

Fukui, Y., Iwata, T., Mizuno, A., Bally, J., & Lane, A. 1993, in *Protostars and Planets III*, ed. E. H. Levy & J. I. Lunine, U. of Arizona Press, p. 497

Ghosh, P. & Lamb, F. K. 1977, ApJ, 217, 578

Ghosh, P. & Lamb, F. K. 1978, ApJ, 223, L83

Heathcote, S., Morse, J., Hartigan, P. Reipurth, B., Bally, J., Schwartz, R. D. & Stone, J. M. 1996, AJ, in press

Gredel, R. & Reipurth, B. 1994, A&A, 289, L19

Herbig, G. H. & Terndrup, D. M. 1986, ApJ, 307, 609

Lada, C. J. 1985, *Ann. Rev. Astron. Astrophys.*, 23, 267

Lada, E. A., Bally, J., & Stark, A. A. 1991a, ApJ, 368, 432

Lada, E. A., DePoy, D. L., Evans, N. J., & Gatley, I. 1991b, ApJ, 371, 171

Lada, E. A., Strom, K. M., & Myers, P. C. 1993 in *Protostars and Planets III*, ed. E. H. Levy & J. I. Lunine, U. of Arizona Press, p. 245

Lovelace, R. V. E., Romanova, M. M., & Bisnovatyi-Kogan, G. S., 1995, MNRAS, 275, 244

McCaughrean, M. J. & Stauffer, J. R. 1994 AJ, 108, 1382

Morse, J. A., Hartigan, P., Heathcote, S., Raymond, J. C. & Cecil, G. 1994, ApJ, 425, 738

O'Dell, C. R., Wen, Z., & Hu, X. 1993, ApJ, 410, 696

O'Dell, C. R. & Wen, Z. 1994, ApJ, 436, 194

Ostriker, E. C. & Shu, F. 1995, ApJ, 447, 813

Raymond, J. 1979, ApJS, 39, 1

Reipurth, B. 1983, A&A, 117, 183

Reipurth, B. 1989, Nature, 340, 42

Reipurth, B. & Olberg, M. 1991, A&A, 246, 535

Reipurth, B., Bally, J., Graham, J. A., Lane, A. P., & Zealey, W. J. 1986, A&A, 164, 51

Reipurth, B. 1994, A General Catalogue of Herbig-Haro Objects, electronically published via anon.ftp to ftp.hq.eso.org, directory /pub/Catalogs/Herbig-Haro

Reipurth, B., Bally, J., & Devine, D. 1996, A&A, in press

Schwartz, R. D. 1975 ApJ, 195, 631

Schwartz, R. D. 1977 ApJS, 35, 161

Shu, F., Najita, J., Galli, D., Ostriker, E., & Lizano, S. 1993, in *Protostars and Planets III*, ed. E. H. Levy & J. I. Lunine, U. of Arizona Press, p. 3

Shu, F., Najita, J., Ostriker, E., Wilken, F., Ruden, S., & Lizano, S. 1994, ApJ, 429, 781

Stone, J. M., Xu, J., & Mundy, L. G. 1995, Nature, 377, 315

Wardle, M. & Königl, A. 1993, ApJ, 410, 218

Winkler, P. F. & Reipurth, B. 1992, ApJ, 389, L25